LETTERS

Neural substrates of awakening probed with optogenetic control of hypocretin neurons

Antoine R. Adamantidis[1]*, Feng Zhang[2]*, Alexander M. Aravanis[2], Karl Deisseroth[1,2] & Luis de Lecea[1]

The neural underpinnings of sleep involve interactions between sleep-promoting areas such as the anterior hypothalamus, and arousal systems located in the posterior hypothalamus, the basal forebrain and the brainstem[1,2]. Hypocretin[3] (Hcrt, also known as orexin[4])-producing neurons in the lateral hypothalamus[5] are important for arousal stability[2], and loss of Hcrt function has been linked to narcolepsy[6–9]. However, it is unknown whether electrical activity arising from Hcrt neurons is sufficient to drive awakening from sleep states or is simply correlated with it. Here we directly probed the impact of Hcrt neuron activity on sleep state transitions with *in vivo* neural photostimulation[10–18], genetically targeting channelrhodopsin-2 to Hcrt cells and using an optical fibre to deliver light deep in the brain, directly into the lateral hypothalamus, of freely moving mice. We found that direct, selective, optogenetic photostimulation of Hcrt neurons increased the probability of transition to wakefulness from either slow wave sleep or rapid eye movement sleep. Notably, photostimulation using 5–30 Hz light pulse trains reduced latency to wakefulness, whereas 1 Hz trains did not. This study establishes a causal relationship between frequency-dependent activity of a genetically defined neural cell type and a specific mammalian behaviour central to clinical conditions and neurobehavioural physiology.

To target genetically expression of channelrhodopsin-2 (ChR2) to Hcrt neurons, we used a lentivirus carrying the 3.1-kilobase (kb) mouse prepro-hypocretin (*Hcrt*, which encodes hypocretin 1 and hypocretin 2) gene promoter[19,20] (Fig. 1a). The specificity of lentivirus-mediated expression was tested by stereotactic delivery of concentrated *Hcrt::ChR2-mCherry* lentiviruses (>10^9 plaque-forming units (p.f.u.) ml^{-1}) into the lateral hypothalamus of *Hcrt::EGFP* transgenic mice[21]. Expression persisted for at least 2 months (Fig. 1b). Out of 748 total enhanced green fluorescent protein (EGFP)-expressing Hcrt cells in the targeted lateral hypothalamus of transduced animals, 658 cells were positive for ChR2–mCherry (87.9 ± 0.9%, Fig. 1c) and ~97% of mCherry-expressing cells also clearly co-expressed EGFP (96.9 ± 1.3%, *n* = 3 animals; Fig. 1c).

To test whether ChR2-expressing Hcrt neurons could precisely respond to light pulses, we used the whole-cell voltage-clamp technique to measure photocurrents in acute lateral hypothalamus brain slices from *Hcrt::EGFP* transgenic mice[21] injected with *Hcrt:: ChR2-mCherry* lentiviruses. Without the addition of any exogenous all-*trans*-retinal[12], all of the cells co-expressing ChR2–mCherry (red) and EGFP (green) in the hypothalamus exhibited photocurrents with a peak amplitude of 182 ± 86 pA (mean ± s.d., *n* = 7 cells; example photocurrent shown in Fig. 1d). In contrast, the occasional EGFP-negative neurons that exhibited dim red fluorescence after virus injection did not respond to blue light under whole-cell patch clamp (*n* = 5 out of 5 cells from 3 animals). In the cells co-expressing EGFP and

mCherry, continuous light illumination for 1 s evoked robust action potential trains under current-clamp conditions (Fig. 1e) with firing frequencies ranging from 8 to 25 Hz. Moreover, as in hippocampal neurons[12], 15-ms blue-light pulses were able to drive reliable action potential trains from 1 to 50 Hz under whole-cell current-clamp conditions (Fig. 1f), although reliability decreased slightly with increasing frequency (Fig. 1g). At 20 Hz, 100% of light pulses gave rise to action potentials, whereas at 50 Hz, 84 ± 14% of light pulses gave rise to action potentials (*n* = 6 cells; Fig. 1g). We found that basal properties including input resistance (366 ± 43 MΩ, *n* = 6)[21] and resting membrane potential were unaltered by ChR2–mCherry expression (*P* > 0.05; Fig. 1h). Together, these data show that lentivirus-mediated expression of ChR2–mCherry in Hcrt neurons is well tolerated, specific and sufficient to drive precise and reliable action potential firing across a range of frequencies.

We next studied the effect of photostimulation of *Hcrt::ChR2-mCherry* neurons on the sleep–wake cycle of freely moving mice. *Hcrt::ChR2-mCherry* or *Hcrt::mCherry* (control) lentiviruses were stereotactically delivered to the lateral hypothalamus; to determine the behavioural consequences of Hcrt neuron activation, we quantitatively analysed sleep recordings of mice chronically implanted with electroencephalographic (EEG) and electromyographic (EMG) electrodes (Fig. 2a). Under baseline conditions, the spontaneous sleep–wake cycle of *Hcrt::ChR2-mCherry* transduced animals was not different from *Hcrt::mCherry* control animals (*P* > 0.05, *n* = 4 animals; Supplementary Fig. 1). We coupled a 200-µm optical fibre to a 20-mW 488-nm diode laser to deliver light into the lateral hypothalamus (Fig. 2a), and fed the optical fibre through the same cannula guide used to deliver the lentiviruses. We measured light scattering in mouse lateral hypothalamus tissue slices (Fig. 2b, c), and estimated that a volume of 0.5 mm^3 received at least 1 mW mm^{-2} (required for ChR2 activation[10]), consistent with the estimated volume of the Hcrt neuronal field (~0.56 mm^3) (Fig. 2c). We found that *in vivo* photostimulation (pulse trains (10 s, 20 Hz) delivered once per minute over 10 min) significantly increased the percentage of Hcrt neurons expressing the c-Fos protein (a marker of neuronal activity) in *Hcrt::ChR2-mCherry* animals compared to the *Hcrt::mCherry* control animals (65.26 ± 4.29% versus 25.72 ± 5.38%, respectively, *P* < 0.01; see Supplementary Fig. 3). This result suggests that *in vivo* photostimulation efficiently activates the Hcrt neuron population.

To test systematically for a causal role of Hcrt neurons in awakening, we next quantitatively measured latency of sleep-to-wake transitions from either slow wave sleep (SWS) or rapid eye movement (REM) sleep in animals transduced with either *Hcrt::ChR2-mCherry* or control lentiviruses (Fig. 3a). On the basis of previous electrical recording of Hcrt neuron activity *in vivo*[22,23], we stimulated each animal with 10 s of light illumination, either in the form of pulsed light flashes (15-ms pulse width) ranging from 1 to 30 Hz,

[1]Department of Psychiatry and Behavioral Sciences, Stanford University, 701B Welch Road, Palo Alto, California 94304, USA. [2]Department of Bioengineering, Stanford University, James H. Clark Center W083, Stanford, California 94305, USA.
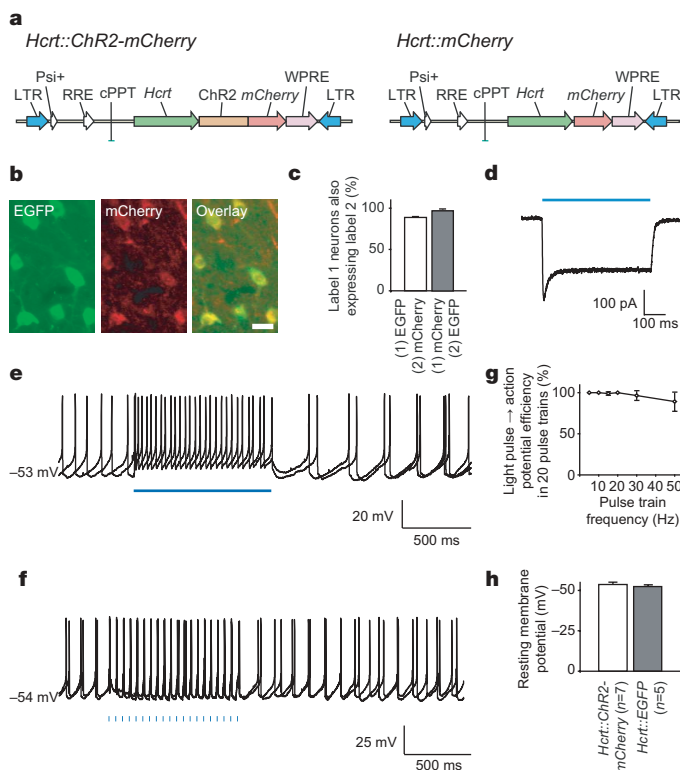*These authors contributed equally to this work.

Figure 1 | Genetically targeted cell-type-specific optical control of Hcrt neurons using ChR2. a, Schematic diagram showing lentiviral vectors carrying the genes for *ChR2-mCherry* or *mCherry* driven by the 3.1-kb mouse *Hcrt* promoter[19,20]. The lentiviral backbone is derived from pLenti-CaMKIIα-ChR2-mCherry[25]. LTR, long terminal repeats; RRE, Rev responsive element; WPRE, woodchuck post-transcriptional regulatory element. **b,** Images of Hcrt neurons (green, *Hcrt::EGFP*) co-expressing ChR2–mCherry protein (red) in the adult mouse lateral hypothalamus (scale bar, 20 μm). Hcrt and mCherry expression was detected by double-fluorescent immunohistochemistry (see Methods). **c,** Lentiviral *Hcrt::ChR2-mCherry* expression is highly specific to the *Hcrt::EGFP* neurons. **d,** *Hcrt::ChR2-mCherry* neurons in the lateral hypothalamus can be electrically controlled with light. Voltage-clamp recording of a neuron expressing ChR2–mCherry in acute lateral hypothalamus slice shows inward photocurrent evoked by illumination with blue light. **e,** Neurons expressing *Hcrt::ChR2-mCherry* in acute lateral hypothalamus brain slices under current-clamp conditions fire action potentials on illumination with 1 s of continuous blue light. Two sweeps are superimposed. **f,** Blue-light pulse trains (15 ms per pulse, 20 Hz) evoked reliable firing of action potential trains. Two consecutive sweeps are superimposed, showing temporal precision of evoked action potential trains even in the presence of basal spontaneous activity (spontaneous activity in Hcrt neurons *in vitro* is expected, as previously reported[29]). Fifteen-millisecond light pulses are indicated by blue bars. **g,** Light-evoked spike trains are reliable over a range of frequencies. The percentage of action potentials evoked by 20 light pulses at the indicated frequency (15–50 Hz) is shown ($n = 6$). **h,** Comparison between the resting membrane potential of ChR2–mCherry/EGFP double-positive ($n = 7$) and EGFP-only ($n = 5$) neurons; ChR2–mCherry expression does not significantly alter basal electrical properties of the Hcrt neurons. Error bars, s.e.m.

or 10 s of continuous illumination. To quantify the effect of each stimulation frequency, we measured the latency between the end of the photostimulation and the next transition to wakefulness (see Methods for description of the sleep–wake cycle criteria used; Fig. 3b, c). Light pulses at 1 Hz did not result in a significant change in latency of SWS or REM sleep to wakefulness in *Hcrt::ChR2-mCherry* animals compared to their controls or their unstimulated baseline recording ($P > 0.05$; Fig. 3b, c). However, photostimulation of Hcrt neurons at frequencies between 5 and 30 Hz during SWS sleep markedly reduced the latency to wakefulness of *Hcrt::ChR2-mCherry* animals compared to control animals ($P < 0.0001$ for all comparisons with control; Fig. 3b and Supplementary Movie 1). Ten-second continuous light stimulation (ON), expected from our *in vitro* work to give rise to >5 Hz firing of the Hcrt neurons, elicited a similar effect ($P < 0.0001$; Fig. 3b). We also systematically studied the

effect of different stimulation frequencies on the latency of REM sleep-to-wake transitions, finding that 5–20 Hz stimulation and constant illumination robustly decreased the latency to wakefulness in *Hcrt::ChR2-mCherry* animals compared to control animals ($P < 0.05$; Fig. 3c and Supplementary Movie 2). Photostimulation effects were consistent not only across frequencies but also across animals, as pooled wake latency values from both SWS and REM sleep for each animal revealed significant differences between experimental and control animals (*Hcrt::mCherry* versus *Hcrt::ChR2-mCherry*: SWS sleep, 57.27 ± 2.67 s and 33.11 ± 2.12 s, respectively (Fig. 4c); REM sleep, 57.90 ± 3.25 s and 30.29 ± 2.88 s, respectively; $P < 0.05$, Student's *t*-test). The Hcrt-neuron-driven latencies to awakening were not fixed; instead, photostimulation shifted the distribution of sleep-to-wake latencies (Fig. 3d, e). Exemplar cumulative probability histograms are shown for 20 Hz and 1 Hz superimposed
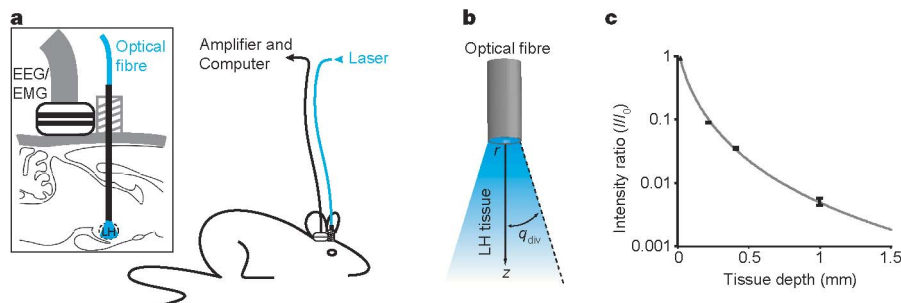

Figure 2 | Integrated *in vivo* optical and physiological system for control of the lateral hypothalamus in the setting of behavioural analysis. a, Schematic of the behavioural set-up used for *in vivo* deep-brain photostimulation in mice. Magnification (inset) shows the EEG/EMG connector used for sleep recording and the cannula guide used for lateral hypothalamus light delivery through an optical fibre. **b,** Schematic of experimental set-up, showing relationship between the optical fibre, brain tissue and attenuating light. *r*, optical fibre radius; *z*, tissue depth from fibre end; q_{div}, the half-angle of divergence. LH, lateral hypothalamus. **c,** Normalized light intensity (mW mm^{-2}) as a function of lateral hypothalamus tissue depth *z*. Values were experimentally determined as previously described[14] by measuring the

light intensity after transmission through a given tissue thickness and dividing by the intensity of the light emanating from the optical fibre tip. Tissue of different thickness was prepared in the form of acute brain slices from adult C57BL/6 mice. Error bars indicate one standard deviation from the mean. Sample size: 0.2 mm, $n = 8$; 0.4 mm, $n = 6$; 1 mm, $n = 2$. Fits were produced using the Kubelka–Munk model of light transmission through diffuse scattering media as previously described[14]. We estimate that by placing the tip of the optical fibre at the upper limit of the lateral hypothalamus, at least 1 mW mm^{-2} of light, which is sufficient to activate ChR2[10], reaches the entire Hcrt field (0.75 mm (medial-lateral) × 0.75 mm (dorso-ventral) × 1 mm (rostro-caudal)).

on respective control distributions, indicating that specific activation of Hcrt neurons increases the probability of awakening from either SWS (Fig. 3d) or REM sleep (Fig. 3e).

Effects of photostimulation seemed to be limited to the sleep-to-wake transition, as durations of the waking events after light delivery were not significantly different between *Hcrt::ChR2-mCherry* and *Hcrt::mCherry* control animals ($P > 0.05$ for each frequency; data not shown). To test further whether Hcrt neuron stimulation specifically modulated arousal state transitions, we developed a semi-chronic photostimulation protocol (pulse trains (10 s, 20 Hz) delivered once per minute over 1 h), and quantified behavioural state transitions and durations during the entire period. We found that this stimulation paradigm increased the number of SWS sleep-to-wake

transitions in *Hcrt::ChR2-mCherry* animals compared to the control animals ($P < 0.05$, two-way analysis of variance (ANOVA) followed by Bonferroni post-hoc tests; Supplementary Table 1) but not total wake, SWS and REM amounts ($P > 0.05$, two-way ANOVA; Supplementary Table 2) or total EEG power characteristics ($P > 0.05$, two-way ANOVA; Supplementary Fig. 2a, b). The relative rarity of REM sleep events (due to the increase in SWS sleep-to-wake transitions) was probably responsible for the absence of change in REM sleep-to-wake transitions in *Hcrt::ChR2-mCherry* animals compared to the control animals in this protocol, as photostimulation was delivered at fixed intervals, independent of vigilance states.

Do these genetically targeted and photosensitized neurons influence neural circuitry via Hcrt release? We administered the Hcrt
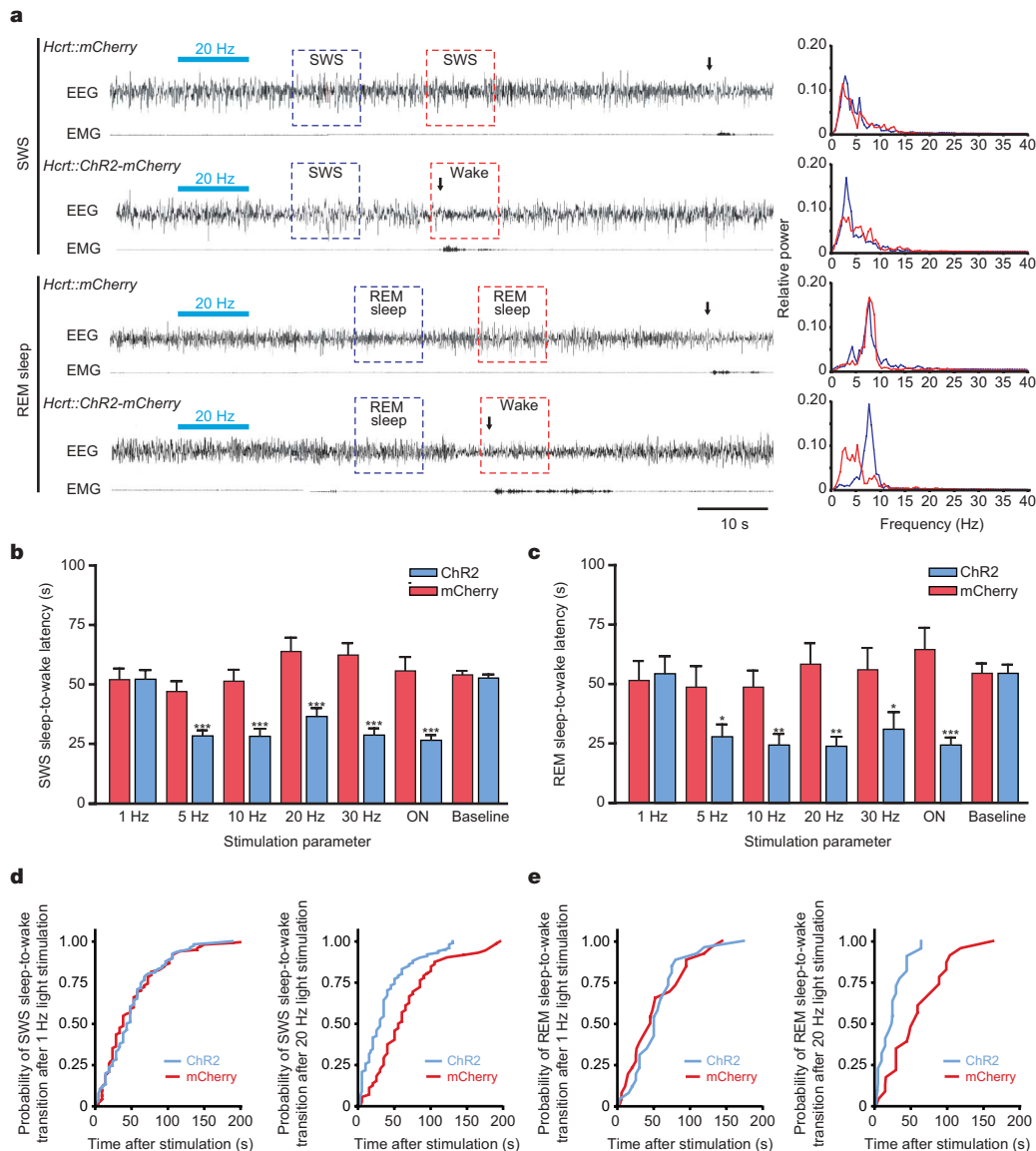

Figure 3 | *In vivo* photostimulation of Hcrt neurons drives sleep-to-wake transitions. a, Representative EEG/EMG recordings showing awakenings after a single bout of photostimulation (15 ms, 20 Hz, 10 s) in *Hcrt::ChR2-mCherry* and *Hcrt::mCherry* (control) animals during SWS (upper traces) and REM sleep (lower traces). Light stimulations are represented by horizontal blue bars. Awakening events are indicated by vertical black arrows according to the described criteria (see Methods). Panels (right) show representative relative cortical EEG power spectra corresponding to the SWS and REM sleep-to-wake transitions highlighted with boxes on the EEG traces (left). **b, c**, Latencies of wake transitions during SWS (**b**) and REM sleep (**c**) of *Hcrt::ChR2-mCherry* transduced animals ($n = 7$) and their controls ($n = 6$) after a single photostimulation bout at different frequencies (15-ms light pulses, at 1–30 Hz,

during 10 s; ON, continuous light illumination of 10 s). Data analysis is based on an average of 15 and 5 stimulations per frequency and per mouse during SWS and REM sleep, respectively. Paired comparison between control conditions for SWS and REM sleep-to-wake transitions did not reveal any significant differences ($P > 0.05$, two-tailed Student's *t*-test). Latencies are represented as mean ± s.e.m. Asterisk, $P < 0.05$; double asterisk, $P < 0.001$; triple asterisk, $P < 0.0001$ using a two-tailed Student's *t*-test between mCherry control (red) and ChR2 animals (blue) for each frequency. **d**, Cumulative probability distribution of latencies from SWS to wakefulness after light stimulation (mCherry control, red curve; ChR2, blue curve). **e**, Cumulative probability distribution of latencies from REM sleep to wakefulness after light stimulation (mCherry control, red curve; ChR2, blue curve).
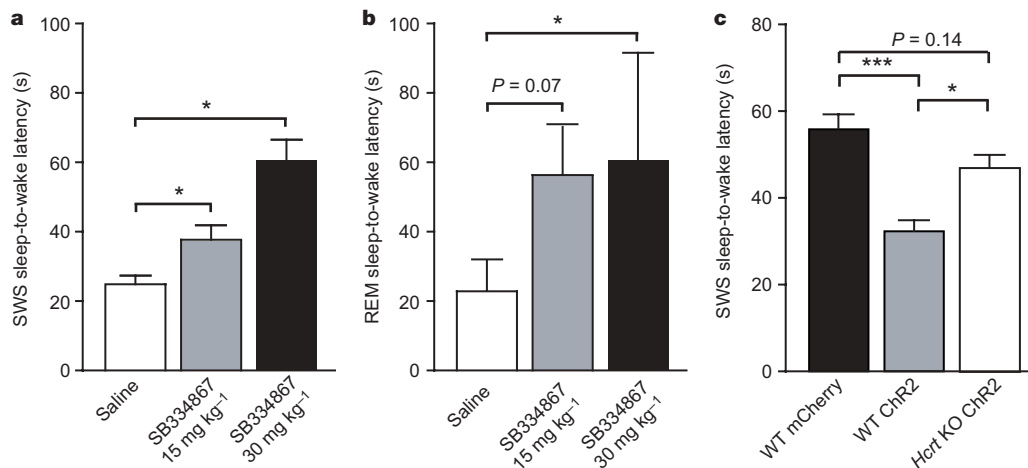
Figure 4 | Behavioural transitions induced by photostimulation are mediated by Hcrt. a, b, Effect of the Hcrt receptor 1 antagonist SB334867 (ref. 24) on latencies of light-induced wake events during SWS (a) and REM sleep (b) in *Hcrt::ChR2-mCherry* transduced animals ($n = 3$) and their controls ($n = 3$) after single bouts of 20 Hz photostimulation (15 ms, 10 s). Data analysis is based on an average of ten and three stimulations per frequency and per mouse for SWS and REM sleep, respectively. At the doses tested here, SB334867 had no effect on the latency of SWS and REM sleep-to-wake transitions after photostimulation in *Hcrt::mCherry* control animals. Latencies are represented as mean ± s.e.m. Asterisk, $P < 0.05$ using a paired Student's *t*-test between saline and drug conditions. **c,** Latencies of SWS sleep-to-wake transitions of *Hcrt* knockout (KO) animals compared with our control data; three independent mice were transduced with *Hcrt::ChR2-mCherry* lentiviruses and received a single photostimulation bout spanning the relevant frequencies (1–30 Hz, 15-ms light pulses, during 10 s). *Hcrt* knockout data analysis is based on an average of 20 stimulations at different frequencies (1–30 Hz) per mouse during SWS. Latencies are represented as pooled mean ± s.e.m. values. Triple asterisk, $P < 0.0001$, indicates the significant difference between control mCherry and ChR2 animals using a two-tailed Student's *t*-test. Asterisk, $P < 0.05$, indicates significant difference using a two-tailed Student's *t*-test between ChR2 and *Hcrt* knockout ChR2 animals. No significant differences in latencies to wakefulness were found between control mCherry and *Hcrt* knockout ChR2 animals.

receptor 1 antagonist SB334867 (ref. 24) 45 min before EEG/EMG recordings and *in vivo* photostimulation with 10-s trains of 20 Hz, 15-ms light pulses. As expected, 20 Hz photostimulation gave rise to brief-latency SWS and REM sleep-to-wake transitions in vehicle-treated animals (Fig. 4a, b). However, administration of a single dose of SB334867 (30 mg kg^{-1}) blocked the photostimulation effect for both SWS and REM sleep-to-wake transitions (Fig. 4a, b; $P < 0.05$, paired *t*-test). A lower dose of the drug (15 mg kg^{-1}) had a similar but reduced effect ($P < 0.05$ for SWS sleep-to-wake transitions; $P = 0.07$ for REM sleep-to-wake transitions, paired Student's *t*-test; Fig. 4a, b, respectively). Furthermore, photostimulations at 5–30 Hz were less effective at reducing SWS sleep-to-wake latencies in *Hcrt::ChR2-mCherry*-transduced *Hcrt* knockout mice compared with wild-type mice (Fig. 4c), demonstrating that Hcrt release is involved in the behavioural effects. However, the effect of photostimulation on wake latency seemed not to be completely blocked in *Hcrt* knockout animals, suggesting a possible role of other neurotransmitters (glutamate, dynorphin) co-expressed in Hcrt neurons.

This study directly establishes a causal link between electrical activity of Hcrt neurons and sleep-to-wake transitions. Using optogenetic technology, we found that we were able to target specifically Hcrt neurons for photostimulation *in vitro*, and that activation of Hcrt neurons at 5 Hz and above (but not at 1 Hz) resulted in a robust decrease in sleep-to-wake latencies from SWS or REM sleep *in vivo*.

Increased probability and number of transitions during repeated stimulation of Hcrt cells suggests a modulatory mechanism by which the Hcrt neural network promotes the initiation of arousal. Hcrt neurons might have additional roles under other conditions than those explored here in many aspects of sleep, including wake maintenance and other arousal-related behaviours. Arousal stability might result from Hcrt activation and divergent modulation of other arousal circuits such as the glutamatergic, cholinergic, histaminergic and dopaminergic systems. The effects seen with even unilateral stimulation suggest that Hcrt neurons have a potent and causal role in driving awakening; bilateral photostimulation could have an even stronger effect on the shortening of sleep-to-wake transitions or arousal maintenance. Dissection of the causal interactions of the

Hcrt system with these other neuromodulatory systems may now be possible with selective control of the Hcrt population. Because Hcrt deficiency results in arousal instability associated with narcolepsy, further insights into sleep disorders may result. Indeed, this demonstration that selective activation of genetically identified neurons can influence a complex behaviour like sleep raises the possibility that this optical technology could be extended to probing the circuit bases of other neurobehavioural and neuropsychiatric disorders.

METHODS SUMMARY

Plasmid and virus preparation. The 3,086-base-pair (*Eco*RI–*Sac*I) mouse *Hcrt* promoter[19,20] was used to replace the CaMKIIα promoter in the *CaMKIIα::ChR2-mCherry* lentivirus vector[25]. The *Hcrt::mCherry* control viruses were made by swapping *ChR2-mCherry* with *mCherry* alone. High-titre lentiviruses were produced as described[25].

Slice preparation and electrophysiology. Recombinant *Hcrt::ChR2-mCherry* lentivirus was stereotactically injected into the lateral hypothalamus (anteroposterior, 1.6 mm; mesolateral, 0.75 mm; dorsoventral, 5.0 mm)[26] of 5–6-week-old *Hcrt::EGFP* mice[21] as described[27]. Coronal slices (250 μm) were prepared and Hcrt neurons were identified via GFP fluorescence and recorded as described[21].

In vivo **light delivery and sleep recordings.** All of the experiments described here were conducted during the same circadian period (12:00–18:00). Each stimulation was applied 15 s after the occurrence of a stable SWS or REM sleep event as detected by online EEG/EMG analysis. Latencies of light-induced sleep-to-wake transitions were measured by off-line scoring of the EEG/EMG recordings as described[28] (see Methods).

Statistical methods. Latencies of sleep-to-wake transitions were analysed using the Student's *t*-test. Pharmacological studies were analysed using a two-tailed paired Student's *t*-test. Two-way ANOVA was used to detect significance in the long-term stimulation experiments.

Full Methods and any associated references are available in the online version of the paper at www.nature.com/nature.

1. Pace-Schott, E. F. & Hobson, J. A. The neurobiology of sleep: genetics, cellular physiology and subcortical networks. *Nature Rev. Neurosci.* **3,** 591–605 (2002).
2. Saper, C. B., Chou, T. C. & Scammell, T. E. The sleep switch: hypothalamic control of sleep and wakefulness. *Trends Neurosci.* **24,** 726–731 (2001).

3. de Lecea, L. *et al.* The hypocretins: hypothalamus-specific peptides with neuroexcitatory activity. *Proc. Natl Acad. Sci. USA* **95**, 322–327 (1998).
4. Sakurai, T. *et al.* Orexins and orexin receptors: a family of hypothalamic neuropeptides and G protein-coupled receptors that regulate feeding behavior. *Cell* **92**, 573–585 (1998).
5. Peyron, C. *et al.* Neurons containing hypocretin (orexin) project to multiple neuronal systems. *J. Neurosci.* **18**, 9996–10015 (1998).
6. Chemelli, R. M. *et al.* Narcolepsy in orexin knockout mice: molecular genetics of sleep regulation. *Cell* **98**, 437–451 (1999).
7. Lin, L. *et al.* The sleep disorder canine narcolepsy is caused by a mutation in the hypocretin (orexin) receptor 2 gene. *Cell* **98**, 365–376 (1999).
8. Peyron, C. *et al.* A mutation in a case of early onset narcolepsy and a generalized absence of hypocretin peptides in human narcoleptic brains. *Nature Med.* **6**, 991–997 (2000).
9. Thannickal, T. C. *et al.* Reduced number of hypocretin neurons in human narcolepsy. *Neuron* **27**, 469–474 (2000).
10. Boyden, E. S., Zhang, F., Bamberg, E., Nagel, G. & Deisseroth, K. Millisecond-timescale, genetically targeted optical control of neural activity. *Nature Neurosci.* **8**, 1263–1268 (2005).
11. Nagel, G. *et al.* Light activation of channelrhodopsin-2 in excitable cells of *Caenorhabditis elegans* triggers rapid behavioral responses. *Curr. Biol.* **15**, 2279–2284 (2005).
12. Zhang, F., Wang, L. P., Boyden, E. S. & Deisseroth, K. Channelrhodopsin-2 and optical control of excitable cells. *Nature Methods* **3**, 785–792 (2006).
13. Lima, S. Q. & Miesenbock, G. Remote control of behavior through genetically targeted photostimulation of neurons. *Cell* **121**, 141–152 (2005).
14. Aravanis, A. M. *et al.* An optical neural interface: *In vivo* control of rodent motor cortex with integrated fiberoptic and optogenetic technology. *J. Neural Eng.* **4**, S143–S156 (2007).
15. Petreanu, L., Huber, D., Sobczyk, A. & Svoboda, K. Channelrhodopsin-2-assisted circuit mapping of long-range callosal projections. *Nature Neurosci.* **10**, 663–668 (2007).
16. Arenkiel, B. R. *et al. In vivo* light-induced activation of neural circuitry in transgenic mice expressing channelrhodopsin-2. *Neuron* **54**, 205–218 (2007).
17. Wang, H. *et al.* High-speed mapping of synaptic connectivity using photostimulation in Channelrhodopsin-2 transgenic mice. *Proc. Natl Acad. Sci. USA* **104**, 8143–8148 (2007).
18. Bi, A. *et al.* Ectopic expression of a microbial-type rhodopsin restores visual responses in mice with photoreceptor degeneration. *Neuron* **50**, 23–33 (2006).
19. Conti, B. *et al.* Transgenic mice with a reduced core body temperature have an increased life span. *Science* **314**, 825–828 (2006).
20. Sakurai, T. *et al.* Structure and function of human prepro-orexin gene. *J. Biol. Chem.* **274**, 17771–17776 (1999).
21. Li, Y., Gao, X. B., Sakurai, T. & van den Pol, A. N. Hypocretin/Orexin excites hypocretin neurons via a local glutamate neuron-A potential mechanism for orchestrating the hypothalamic arousal system. *Neuron* **36**, 1169–1181 (2002).
22. Lee, M. G., Hassani, O. K. & Jones, B. E. Discharge of identified orexin/hypocretin neurons across the sleep–waking cycle. *J. Neurosci.* **25**, 6716–6720 (2005).
23. Mileykovskiy, B. Y., Kiyashchenko, L. I. & Siegel, J. M. Behavioral correlates of activity in identified hypocretin/orexin neurons. *Neuron* **46**, 787–798 (2005).
24. Smart, D. *et al.* SB-334867-A: the first selective orexin-1 receptor antagonist. *Br. J. Pharmacol.* **132**, 1179–1182 (2001).
25. Zhang, F. *et al.* Multimodal fast optical interrogation of neural circuitry. *Nature* **446**, 633–639 (2007).
26. Paxinos, G. & Franklin, K. *The Mouse Brain in Stereotaxic Coordinates* 2nd edn (Academic, New York, 2001).
27. Cetin, A., Komai, S., Eliava, M., Seeburg, P. H. & Osten, P. Stereotaxic gene delivery in the rodent brain. *Nature Protocols* **1**, 3166–3173 (2006).
28. Bourgin, P. *et al.* Hypocretin-1 modulates rapid eye movement sleep through activation of locus coeruleus neurons. *J. Neurosci.* **20**, 7760–7765 (2000).
29. Eggermann, E. *et al.* The wake-promoting hypocretin-orexin neurons are in an intrinsic state of membrane depolarization. *J. Neurosci.* **23**, 1557–1562 (2003).

METHODS

Animals. Mice were housed in individual plexiglass recording cages in temperature- ($22 \pm 1\,°C$) and humidity (40–60%)-controlled recording chambers (custom-designed stainless steel cabinets with individual ventilated compartments) under a 12 h/12 h light/dark cycle (starting at 7:00). Food and water were available *ad libitum*. All the experiments were carried out in accordance with the guidelines described in the National Institutes of Health Guide for the Care and Use of Laboratory Animals.

Immunocytochemistry. To verify the phenotype of neurons that expressed the ChR2–mCherry fusion protein, infused transgenic *Hcrt::EGFP* mice were anaesthetized with isofluorane and perfused transcardially with physiological saline followed by 4% paraformaldehyde in PBS (pH 7.4). The brains were dissected out and post-fixed in the same fixative overnight at $4\,°C$ and finally cryoprotected in 30% sucrose dissolved in PBS for 48 h at $4\,°C$. Thirty-micrometre coronal sections containing the lateral hypothalamus were washed in phosphate-buffered saline (PBS; pH 7.4), treated with 0.3% Triton X-100 (PBST), and immersed in a blocking solution consisting of 4% bovine serum albumin dissolved in PBS. Some sections were immunostained with rabbit antiserum against DsRed proteins (1:1,000; Clontech). A secondary anti-rabbit immunoglobulin conjugated to biotin was used before an amplification of the signal using the ABC kit (Vector) and TSA kit (NEN Life Science Products). Briefly, sections were washed in PBST for 3×10 min, and incubated for 1 h at room temperature with an anti-rabbit biotinylated conjugate diluted in PBST. Sections were then washed three times in PBST and incubated with the TSA kit for 15 min. After washes, sections were finally incubated with a streptavidin–Alexa-fluor 596 conjugate (Molecular Probes) diluted 1:1,000 in PBST for 1 h at room temperature.

c-Fos and Hcrt double immunostaining was performed on brain sections from *Hcrt::ChR2* and *Hcrt::mCherry* transduced animals ($n = 5$ and 6, respectively). Briefly, 2–3 weeks after lentivirus injection, animals were photostimulated (light pulse trains of 10 s at 20 Hz every minute for 10 min) and perfused 1 h after stimuli. Brains were post-fixed and cryoprotected as described above. Coronal brain sections containing the lateral hypothalamus were successively incubated in (1) a rabbit antiserum to c-Fos (1:1,000, Calbiochem) in PBST supplemented with 4% bovine serum albumin (BSA, Sigma) for 1 day at $4\,°C$; (2) a biotinylated anti-rabbit IgG solution (1:1,000, Vector Laboratories) in PBST; and (3) an ABC-peroxidase solution (1:1,000, Vector Laboratories) both for 60 min at room temperature. Finally, sections were stained using 3,3′-diaminobenzidine-4 HCl and nickel solution (DAB-Ni; Vector Laboratories) to obtain dark-purple staining. Four washes in phosphate buffer were performed between each step. The c-Fos-stained sections were incubated in a goat antiserum to Hcrt (1:5,000; Santa Cruz) in PBST/BSA 4% for 2 days at $4\,°C$. Amplification steps were similar to those described above but the final step was performed in DAB solution without nickel to obtain brown staining. Finally, the sections were mounted on slides, dried and coverslipped with permaslip.

Sections were washed, mounted and coverslipped, and examined with a fluorescence microscope (Carl Zeiss). Digital images from the microscopy were slightly modified to optimize for image resolution, brightness and contrast in Adobe Photoshop 7.0 (Adobe Systems), to represent optimally the immunohistochemistry observed.

Hcrt-positive and Hcrt-positive/c-Fos-positive neurons were counted in each hypothalamic structure (within both ipsilateral and contralateral sides of injection site) present on at least four Hcrt/c-Fos double-labelled sections for each animal. Lateral hypothalamus coronal section maps were made according to the mouse brain atlas[26] to represent the placement of the cannula guide in each animal.

Polysomnographic recording and analysis. For sleep–wake cycle recording, the EEG signals were recorded from two electrodes placed on the frontal (AP, -2; ML, ±1) and temporal (AP, 3; ML, ±2.5) cortices. Two wire electrodes were inserted in the neck musculature to record postural tone through EMG activity. Insulated leads from the EEG and EMG electrodes were then soldered to a miniconnector that was cemented to the skull with meta-bond (Parkell) and dental acrylic. Mice were housed individually for at least 10 days after surgery and were then connected to commutators with flexible cables for habituation to the EEG/EMG recording conditions. Cortical EEG and EMG signals were amplified using Grass Instruments (West Warwick) and digitized at 256 Hz using a sleep recording system (VitalRecorder, Kissei Comtec). The signals were digitally filtered and spectrally analysed by fast Fourier transform (represented in Fig. 3a, right panels), and polysomnographic recordings were visually scored by 5-s epochs for wake, SWS and REM sleep, as previously described[28]. The following criteria were used. Wakefulness is characterized by desynchronized low-amplitude EEG and EMG activity with phasic bursts. SWS is characterized by synchronized, high-amplitude, low-frequency (0.25–4 Hz) EEG and reduced EMG activity compared to wakefulness. A decrease in the EEG amplitude associated with a flat EMG (muscle atonia) and a regular and pronounced theta rhythm (4–9 Hz) signalled the onset of REM sleep episodes. Sleep state changes were recorded when at least one epoch in a different sleep stage was scored. SWS and REM sleep-to-wake transition latencies were calculated as the time from the end of the light stimulation (during SWS or REM sleep) to the first event of wakefulness. Awakenings occurring during photostimulation were discarded from the analysis. The EEG power densities obtained for each state were summed over the frequency band of 0.5–40 Hz (total power). To normalize the data, all power spectral densities at the different frequency ranges, that is, delta (0.5–4 Hz), theta (4.5–9 Hz), alpha (9–15 Hz), were expressed as relative values to the total power of the same epochs. Four-second epochs with more than two vigilance states were omitted from the EEG power analysis. The full sleep–wake cycle of mice is very short compared to human (2–3 min). Consequently, based on the EEG/EMG precise criteria and power spectrum analysis of the EEG, mice show sleep epochs between 5 and 250 s in duration, with an average of 50 s during spontaneous sleep.

Optical fibres were placed 1 h before experiments (11:00) and removed immediately afterwards (18:00). Light pulse trains (1–30 Hz) were programmed using a function generator (33220A, Agilent Technologies). For each animal, spontaneous sleep–wake cycles as well as light-induced sleep-to-wake transitions were characterized. In a first set of experiments, we measured latencies of light-induced sleep-to-wake transitions at different frequencies (1–30 Hz and 10 s continuous illumination). In a second series of experiments, specificity of the activation of Hcrt neural network on the light-induced SWS and REM sleep-to-wake transitions was assessed by administration of the Hcrt receptor 1 antagonist (SB334867, Tocris) before photostimulation (15 ms light pulses at 20 Hz during 10 s). Latency to wakefulness was measured as previously described. In a third series of experiments, we used an automated long-term stimulation protocol (15 ms light pulses at 20 Hz for 10 s every minute during 1 h) to test the behavioural consequences of sustained stimulations of the Hcrt neural network. The sleep–wake cycle parameters (wake, SWS, REM sleep duration and behavioural transitions) were then quantified by off-line scoring of the entire hour of stimulation and the corresponding circadian baseline for each animal. Polysomnographic scoring was performed blindly by two scorers and was found to lie within a 95% confidence interval (κ coefficient = 0.840).